Molecular Therapy
Methods & Clinical Development
Original Article

In vivo PCSK9 gene editing using an all-in-one self-cleavage AAV-CRISPR system

Qian Li,[1,2] Jing Su,[1,2] Yi Liu,[1] Xiu Jin,[1] Xiaomei Zhong,[1] Li Mo,[1] Qingnan Wang,[1] Hongxin Deng,[1] and Yang Yang[1]

[1]State Key Laboratory of Biotherapy and Cancer Center, West China Hospital, Sichuan University and Collaborative Innovation Center, Chengdu 610041, China

Adeno-associated virus (AAV)-mediated delivery of the clustered regularly interspaced short palindromic repeat-CRISPR-associated protein 9 (CRISPR-Cas9) has shown promising results in preclinical models. However, the long-term expression of Cas9 mediated by AAV in the post-mitotic cells raises concerns with specificity and immunogenicity. Thus, it would be advantageous to limit the duration of Cas9 expression following delivery. In this study, we have engineered an all-in-one self-cleavage AAV-CRISPR-Cas9 system to restrict the expression of Cas9 nuclease, which consists of a Cas9 nuclease from Staphylococcus aureus (SaCas9), a chimeric single guide RNA (sgRNA) molecule targeting *PCSK9*, and flanking sites targeted by this sgRNA. The self-cleavage system generated a negative feedback loop where Cas9 cut both the target genomic locus and the AAV vector, thus self-limiting the expression of Cas9. We demonstrated that this system could reduce ~60% expression of SaCas9 protein and had a 20-fold reduction in off-target activity at 24 weeks post-vector administration *in vivo*. Moreover, the on-target editing efficacy was not compromised and resulted in a stable reduction in circulating PCSK9 and serum cholesterol. The inclusion of this self-cleavage system in gene-editing approaches could increase the safety profile of AAV-delivered genome-editing nucleases and thereby promote its clinical transformation.

INTRODUCTION

The clustered regularly interspaced short palindromic repeat-CRISPR-associated protein 9 (CRISPR-Cas9) system is a powerful technology for genome editing and gene-expression control.[1] The Cas9 nuclease could direct to a specific genomic region cleaving the DNA target sequence with a single guide RNA (sgRNA).[2,3] Especially, the presence of a protospacer adjacent motif (PAM) in the target DNA is strictly required for sgRNA-guided DNA recognition and cleavage.[4,5] This system has great potential for both basic research and clinical applications because of its simplicity, high efficiency, design flexibility, and multiplex targeting capacity.[6,7] It has been widely used in diverse fields of medical research, biotechnology, and agriculture. Safe and efficient delivery of CRISPR-Cas9 *in vivo* remains the key challenge for its applications in disease treatments. At present, adeno-associated virus (AAV)-mediated delivery of the CRISPR-Cas9 system has shown high gene targeting efficacy *in vivo*. AAV has low immunogenicity and serotype specificity, which can safely deliver the CRISPR-Cas9 system to various cell types, tissues, and organs.[8–10] It has been reported that AAV-based CRISPR-Cas9 therapeutic genome editing has been used in numerous studies involving disease animal models and patients.[11] The successful applications of AAV vectors in gene therapy promoted their adoption for clinical trials. However, AAV vectors genome can largely remain as stable episomes inside host cells. They can mediate long-term transgene expression in post-mitotic cells and lead to long-term therapeutic efficacy. But in many genome editing applications, it is not necessary for permanent expression of an active genome-editing system. It has been shown that the long-term expression of Cas9 in target cells can pose a safety concern such as cytotoxicity, off-target risks, and immune responses *in vivo*.[12–14] Thus, it would be advantageous to limit the duration of Cas9 nuclease expression following delivery for clinical therapeutic research.

Proprotein convertase subtilisin/kexin type 9 (PCSK9) specifically expressed and secreted from the liver and bound to low-density lipoprotein receptor (LDLR). It has been reported that the loss-of-function mutations in *PCSK9* can significantly reduce the levels of LDL cholesterol (LDL-C) and coronary heart disease risks.[15,16] Inhibition of *PCSK9* using CRISPR-Cas9 for the treatment of cardiovascular disease has achieved a reduction of serum cholesterol.[17–20] In the present study, we developed a self-cleavage AAV-CRISPR-Cas9 system that consists of a Cas9 nuclease from Staphylococcus aureus (SaCas9), a chimeric sgRNA molecule targeting *PCSK9*, and flanking sites targeted by this sgRNA. We demonstrated that this system can effectively eliminate SaCas9 protein expression without compromising on-target efficacy and significantly reduce the off-target effect and immune effect of CRISPR-Cas9 *in vivo*. Introducing this self-cleavage strategy in gene-editing approaches has the potential to enhance the safety profile of AAV-delivered genome-editing nucleases and thereby address the concerns with therapeutic applications of AAV-mediated CRISPR-Cas9 system.

Received 28 July 2020; accepted 3 February 2021;
https://doi.org/10.1016/j.omtm.2021.02.005.

[2]These authors contributed equally

Correspondence: Yang Yang, State Key Laboratory of Biotherapy and Cancer Center, West China Hospital, Sichuan University and Collaborative Innovation Center, Chengdu 610041, China.
E-mail: yang2012@scu.edu.cn

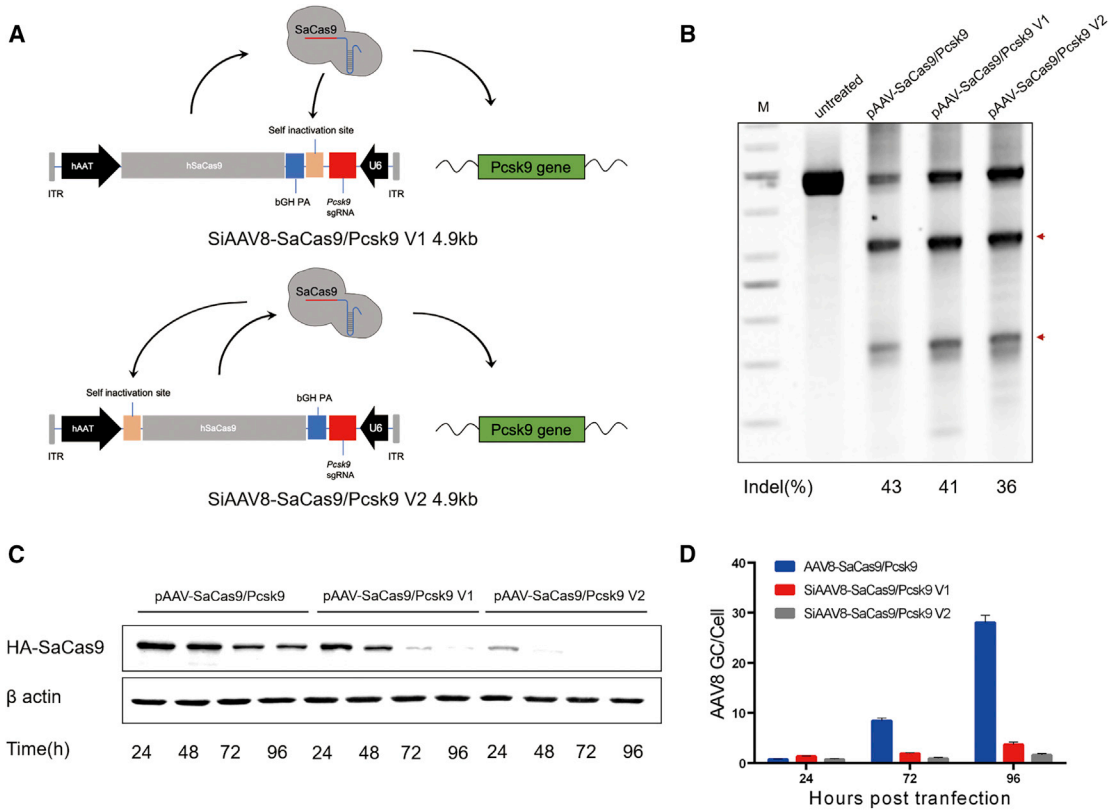

Figure 1. Construction and comparison of self-cleavage vectors *in vitro*

(A) Schematic illustrating self-cleavage AAV-CRISPR-Cas9 systems. (B) *In vitro* validation of self-cleavage plasmids in the H2.35 mouse cell line by transient transfection and SURVEYOR nuclease assays. Arrows represent SURVEYOR nuclease cleaved fragments of the *PCSK9* PCR products. (C) Western blot analysis. Cell lysates were prepared at different time points from H2.35 mouse cell line transiently transfected with self-cleavage candidates or control vectors for detection of SaCas9 protein. (D) Quantitative analysis of virus genome copy number at different time points after infection with Huh7 cell line by qPCR. Mean ± SEM are shown.

RESULTS

Construction and evaluation of self-cleavage AAV-CRISPR-Cas9 vectors *in vitro*

We designed and engineered 3 sgRNAs (Table S1) targeting *PCSK9* exon 3 and confirmed their activities *in vitro* in the murine cell line H2.35 without puromycin selection, via SURVEYOR nuclease assays. The sgRNA2 demonstrated a higher on-target editing efficiency (~18%) than other sgRNAs (Figure S1). The pAAV-SaCas9/Pcsk9 plasmid, which consists of a liver-specific human alpha 1-antitrypsin(hAAT) promoter, SaCas9, and an U6-*PCSK9* sgRNA2, was constructed for subsequent studies as a control. To develop a self-cleavage AAV-CRISPR platform, we designed two strategies, which add self-cleavage sequences (*PCSK9* target sequence and PAM sequence) at different positions of the vector (Figure 1A). The self-cleavage sequence was inserted between SaCas9 and sgRNA expression cassettes in the pAAV-SaCas9/Pcsk9 V1 plasmid, while the self-cleavage sequence was placed between the SaCas9 coding sequence and the hAAT promoter in the pAAV-SaCas9/Pcsk9 V2 plasmid.

In order to select the optimal self-cleavage vector for *in vivo* animal experiments, we evaluated the genome-editing efficiency and Cas9 protein expression of the two candidate plasmid vectors *in vitro*. The plasmids were transfected into the H2.35 cell line and selected by puromycin, in which the parental pAAV-SaCas9/Pcsk9 plasmid vector was used as a positive control. SURVEYOR nuclease assays showed that the genome-editing efficiency of pAAV-SaCas9/Pcsk9, pAAV-SaCas9/Pcsk9 V1, and pAAV-SaCas9/Pcsk9 V2 groups was 43%, 41%, and 36%, respectively (Figure 1B). Next, the cells were collected at 24 h, 48 h, 72 h, and 96 h after transfection, and the total cell protein was extracted for western blot (WB) to detect the expression of Cas9 protein. The results showed that the expression of Cas9 protein in both pAAV-SaCas9/Pcsk9 V1 and pAAV-SaCas9/Pcsk9 V2 group decreased significantly with time (Figure 1C). In addition, AAV8 virus was packaged and used to infect the Huh7 cell, HCCLM3 cell, and SMCC-7721 cell. Then, genomic DNA was extracted at 24 h, 72 h, and 96 h after infection, and the genome copy number of AAV8 in cells was detected by qPCR. The qPCR results showed that the genome copy number of virus in both SiAAV8-SaCas9/Pcsk9 V1 and SiAAV8-SaCas9/Pcsk9 V2 group increased slowly with time (Figure 1D; Figure S2). The SiAAV8-SaCas9/Pcsk9 V1 had the highest on-target activity and was selected for further testing *in vivo*.

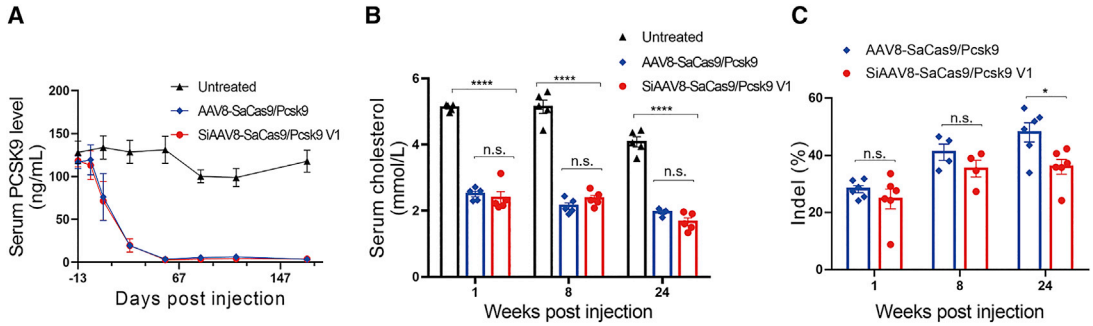

Figure 2. Editing of *PCSK9* target with self-cleavage AAV-CRISPR system *in vivo*

(A) Time course of serum PCSK9 was measured by ELISA following tail vein injections of 4- to 6-week-old male C57/BL6 mice with the SiAAV8-SaCas9/Pcsk9 V1 or AAV8-SaCas9/Pcsk9 (2×10^{11} GC/mouse). Untreated C57/BL6 mice (n = 5) were included as control. (B) Time course of serum total cholesterol level. (C) Indel frequency at different time points in treated mice. Mean ± SEM are shown. *p < 0.05, ****p < 0.0001, Dunnett's test. ns, non-significant.

The self-cleavage AAV-CRISPR-Cas9 system could effectively edit *PCSK9 in vivo*

To evaluate the genome-editing efficacy of this self-cleavage system *in vivo*, we injected 2×10^{11} genome copies (GCs) of AAV8-SaCas9/Pcsk9 and SiAAV8-SaCas9/Pcsk9 V1 into 4- to 6-week-old C57/BL6J male mice via tail vein injection, respectively. We first detected the expression of PCSK9 protein and the total cholesterol in the serum of mice. We found that serum PCSK9 decreased by approximately 80% and total cholesterol decreased by approximately 35% after 24 weeks of administration. Moreover, there was no significant difference between the SiAAV8-SaCas9/Pcsk9 V1 targeting group and the control AAV8-SaCas9/Pcsk9 targeting group (Figures 2A and 2B). In addition, we sacrificed mice at 1, 8, and 24 weeks post injection and harvested liver samples to evaluate the genome-editing efficiency by SURVEYOR nuclease assays. The results showed that the cleavage frequencies of the two groups ranged from 25% to 45% (Figure 2C). These results demonstrated that the on-target editing efficacy of the self-cleavage AAV8-CRISPR-Cas9 system was comparable to that obtained with the parental AAV-SaCas9/Pcsk9 system. Though the genome editing efficiency of the self-cleavage AAV8-CRISPR-Cas9 targeting group slightly decreased at 24 weeks after injection, the reduction of PCSK9 protein and total cholesterol were not significant when compared with the parental AAV8-SaCas9/Pcsk9 targeting group.

The self-cleavage AAV-CRISPR-Cas9 system reduced Cas9 expression and AAV8 genome copy in the liver

To further analyze the self-cleavage system, we first compared the expression of SaCas9 protein and the genome copy number of AAV8 in liver tissue at 1, 8, and 24 weeks post injection. Western blot and qPCR results showed that the SiAAV8-SaCas9/Pcsk9 V1 targeting group had a significant reduction of Cas9 protein and viral genome copy number with time (Figures 3A and 3B). The expression of Cas9 protein decreased by about 60%, and the viral genome copy number decreased by about 70% at 24 weeks after injection when compared with the parental AAV8-SaCas9/Pcsk9 targeting group.

The self-cleavage AAV-CRISPR-Cas9 system improved the safety profile of genome editing

Next, we evaluated the off-target activity *in vivo*. The algorithm described in https://www.benchling.com/ identified 49 potential off-target sites for sgRNA2. The top 10 sites that are most likely to create double-stranded breaks (DSBs) were amplified by PCR and deep sequenced (Table S2). The PCR amplicons were generated by nested PCR on liver genomic DNA extracted at 24 weeks post viral injection. The indels in the PCR amplicons were quantified via next generation sequencing (NGS). The results showed that mice treated with SiAAV8-SaCas9/Pcsk9 V1 had a 20-fold reduction in off-target activity compared with the AAV8-SaCas9/Pcsk9-treated group (Figure 3C). Finally, we detected neutralizing antibodies against AAV8 capsid and SaCas9 protein in mice serum by ELISA. The results showed that both groups of mice produced neutralizing antibodies against AAV8 capsid and SaCas9 protein at 8 and 24 weeks, respectively. The SiAAV8-SaCas9/Pcsk9 V1 targeting group had lower antibody levels than the AAV8-SaCas9/Pcsk9 targeting group (Figures 3D and 3E). Among them, there was a significant difference in Cas9 antibody, but there was no significant difference in AAV neutralizing antibody. Thus, the self-inactivating AAV8-CRISPR-Cas9 system can effectively reduce Cas9 expression and significantly reduce the off-target effect and immune effect of CRISPR-Cas9 *in vivo*.

Toxicity evaluation of self-cleavage system

We performed a histological examination of the mouse liver tissues. In the hematoxylin and eosin (H&E) staining results, no signs of inflammation such as aggregates of lymphocytes or macrophages were detected (Figure 4A). In addition, we evaluated the serum level of aspartate aminotransferase (AST) and alanine aminotransferase (ALT). The results showed that compared with the untreated group, neither the SiAAV8-SaCas9/Pcsk9 targeting group nor the AAV8-SaCas9/Pcsk9 targeting group showed a toxicity effect (Figures 4B and 4C).

Self-cleavage AAV vector integrates into the genomic loci and generates indels in the AAV genome

Previous studies have shown that a fraction of AAV vectors are integrated into pre-existing DSBs.[21] Thus, we designed an experiment to

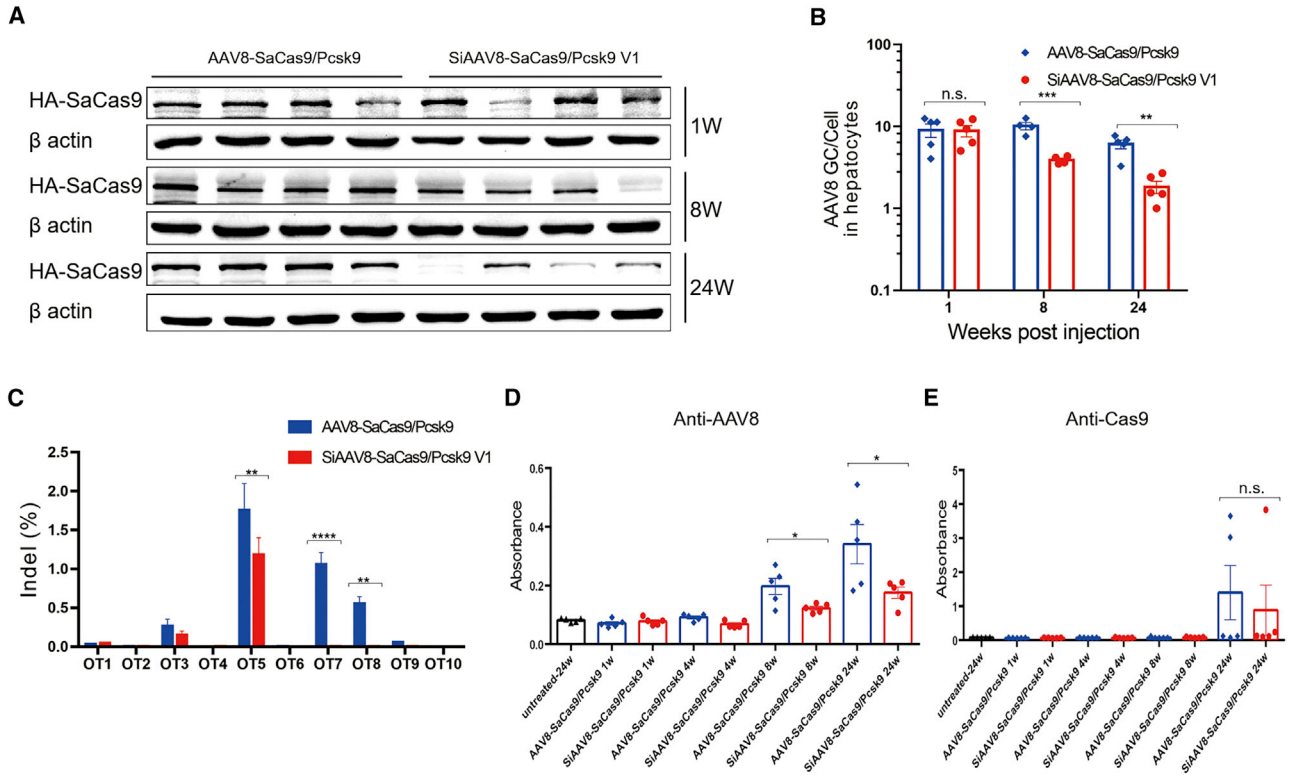

Figure 3. Evaluation of self-cleavage AAV-CRISPR system *in vivo*

(A) Western blot analysis. Liver lysates were prepared at 1, 8, and 24 weeks post-injection for detection of SaCas9 protein. (B) Quantitative analysis of virus genome copy number in liver tissue at 1, 8, and 24 weeks post-injection by qPCR. (C) Deep sequencing data of off-target sites of liver DNA samples isolated from 24 weeks post-injection mice. (D) Immune responses of treated mice were detected by ELISA for the AAV8 virus capsid. (E) Immune responses of treated mice were detected by ELISA for SaCas9 protein. Mean ± SEM are shown. *$p < 0.05$, **$p < 0.01$, ***$p < 0.001$, ****$p < 0.0001$, Dunnett's test.

examine possible vector insertions with the self-cleavage system. We performed PCR using primers (Table S4) at the 5′ end of the *PCSK9* cleavage site to check for possible vector insertions (Figure 5A). We detected the integration of AAV at the genomic loci in all AAV-injected animals. However, the amplicons of samples injected with self-cleavage AAV vectors had full-length AAV amplification bands and truncated AAV fragments (Figure 5B). Integration of the truncated AAV fragments illustrates that the AAV vectors did indeed undergo self-cleavage. Moreover, we also performed PCR on the cleavage site of the AAV self-cleavage vectors and detected that about 30% of the indels occurred in the self-cleavage AAV vectors at 1, 8, and 24 weeks by NGS (Figure 5C). Overall, consistent with previous studies,[22] our data indicate that AAV integration at the on-target cut site is a major gene-editing outcome *in vivo* and should be carefully evaluated in the future clinical development.

DISCUSSION

Here, we designed an all-in-one self-cleavage AAV-CRISPR-Cas9 technology to limit the long-term expression of Cas9 nuclease. We demonstrated that the self-cleavage system could significantly reduce Cas9 protein expression without compromising on-target efficacy *in vitro* and *in vivo*. Moreover, the results showed that the risk of off-target response and humoral immune response to AAV8 capsid protein was significantly reduced. We proved that the self-cleavage gene-editing approaches have the potential to circumvent problems related to permanent Cas9 expression, achieving safe and efficient genome editing.

Recently, several methods to control the activity of Cas9 have been developed, such as nuclease splitting, chemically controlling protein stability or other inducible systems.[23–26] It has been reported that doxycycline-regulated Cas9 induction can limit the duration of Cas9 expression.[27] Besides, small phage-encoded anti-CRISPR proteins to inactivate Cas9 also have been reported.[28] However, these approaches rely on using non-human protein moieties to control Cas9 activity, which will cause other safety risks. Therefore, it is necessary to find a safer and more effective methods to limit the long-term expression of Cas9 nuclease.

In this study, according to the mechanism of CRISPR-Cas9, we designed two self-cleavage strategies to limit the duration of Cas9 expression by adding self-cleavage sequences (*PCSK9* target sequence and PAM sequence) at different positions of the vector (Figure 1A). We compared the two candidate plasmid vectors *in vitro* and found that the genome-editing efficiency of pAAV-SaCas9/Pcsk9 V1 is higher

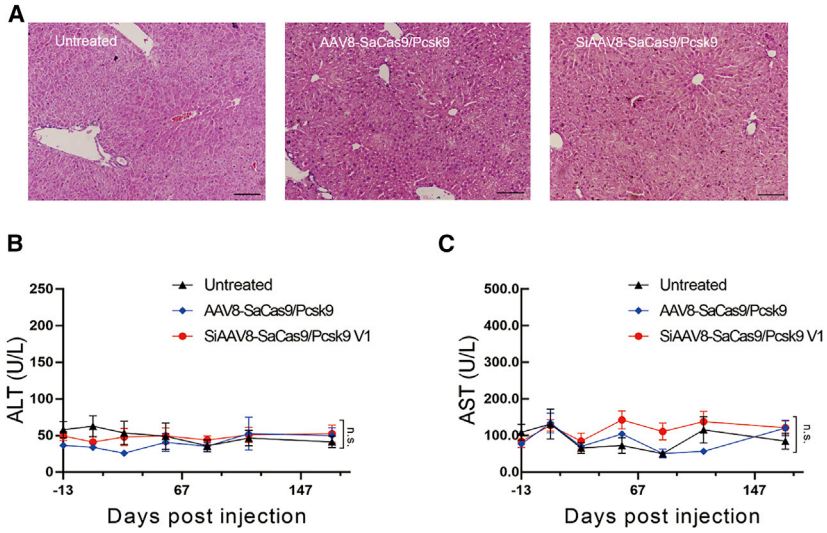

Figure 4. Liver function tests and toxicity examination

(A) Liver histological analysis was performed with H&E staining at 24 weeks after injection. Scale bar, 100 μm. (B and C) Liver function tests in *PCSK9*-targeted (both SiAAV8-SaCas9/Pcsk9 and AAV8-SaCas9/Pcsk9, n = 5) and uninjected (n = 5) animals. Mean ± SEM are shown. Dunnett's test.

and it can eliminate more than 90% of its expression of Cas9 protein within 72 h. Although the self-cleavage effect of pAAV-SaCas9/Pcsk9 V2 is better, it has lower genome-editing efficiency, which might be due to a faster self-inactivating rate (Figures 1B and 1C). It is interesting to note that the expression of Cas9 protein was lower after 24 h when using pAAV-SaCas9/Pcsk9 V2. We speculate that it may be not only due to self-cleavage mechanisms but also because the cleavage site is placed in the 5′ UTR,[29] which affects the expression of Cas9. According to these results, we finally chose to package AAV8 virus with pAAV-SaCas9/Pcsk9 V1 for *in vivo* animal study.

Similar self-inactivating systems in gene-editing approaches such as "KamiCas9" and "Lenti-SLiCES" have been used to eliminate the expression of Cas9 protein *in vivo*.[30,31] However, the two systems require multiple vectors or sgRNAs to achieve self-cleavage and the delivery of them via lentiviral vectors has risks associated with random integration into the host genome, which will increase the possibility of host carcinogenesis.[32] AAV has low immunogenicity, high safety, and tissue tropism, so it is widely used for delivery of CRISPR-Cas9 system to various tissues, such as the liver, muscle, heart, and brain.[33] A similar self-deleting AAV-CRISPR system using a CRISPR sgRNA that cuts the Cas9 coding sequence *in vivo* has been reported.[33] The system relies on co-transduction with two AAV vectors to achieve self-deletion. Although the Cas9 expression AAV vector was destroyed, another sgRNA expression AAV vector remained intact to express sgRNA. Our all-in-one vector system can effectively reduce Cas9 protein expression with time in the majority of hepatocytes while maintaining efficient *in vivo* editing of *PCSK9* target. Although the target efficiency slightly decreased at 24 weeks post injection (Figure 2C), the self-cleavage system can reduce the serum level of PCSK9 protein and total cholesterol with no significant difference from the parental system (Figures 2A and 2B). The results indicated that durable therapeutic effects could be achieved as long as most of the permanent edited hepatocytes survive or expand. Compared with the dual AAV system, an all-in-one vector system would be preferred, which would ensure simultaneous delivery of Cas9 and self-cleavage sgRNA into the same cells.[33] In addition, an all-in-one vector system can reduce the injection dose of viral vectors and humoral immune response to AAV capsid, which has the potential for clinical application.[34]

In our study, the decreased Cas9 expression is accompanied with lower AAV genome copy per cell. In designing this approach, we intended to inactivate AAV episomes with Cas9 to facilitate their degradation. However, the specific mechanism of the reduction of the AAV vectors and Cas9 protein is not clear. We detected the integration of full-length and truncated AAV vectors at genomic loci (Figures 5A and 5B) and also found that the self-inactivating virus produces about 30% of indels in the AAV genome (Figure 5C). The results indicated that not all AAV vectors could occur at non-homologous end joining (NHEJ) after cleavage; some might be integrated into the vector or genomic loci and some might be degraded after inactivation, resulting in a reduction of AAV genome copy number. In addition, inactivated mutations introduced in the AAV genome could effectively silence transgenic expression and reduce the expression of Cas9 protein.[33]

Previous studies have observed that the long-term expression mediated by AAV delivery of Cas9 nuclease to post-mitotic cells raises concerns with off-target cleavage, cytotoxicity, and immunogenicity, which greatly limits the therapeutic applications of AAV-CRISPR-Cas9.[35] Consistent with previous self-cleavage reports,[33] SaCas9 cannot be completely removed. Our self-cleavage system still has 40% expression of SaCas9 protein 24 weeks after injection in mice, which might limit the application of this technology. However, we analyzed the off-target effect via NGS in the predicted regions and found that the self-cleavage AAV8-CRISPR-Cas9 system has a 20-fold reduction in off-target activity at 24 weeks after AAV administration (Figure 3C). Besides, it has been found that humoral immune response to AAV8 capsid protein and Cas9 protein exists in humans and mice.[36,37] ELISA results showed that the self-cleavage AAV8-CRISPR-Cas9 system can reduce the humoral immune response (Figures 3D and 3E). Meanwhile, mice treated with AAV revealed no abnormal liver function (Figure 4A). Detailed analysis of transaminase levels, which contains AST and ALT, did not show a toxicity effect (Figures 4B and 4C). These results suggested that the self-cleavage AAV8-CRISPR-Cas9 system could greatly improve its safety in applications by reducing the risk of off-target response and humoral immune response to AAV8 capsid protein and Cas9 protein.

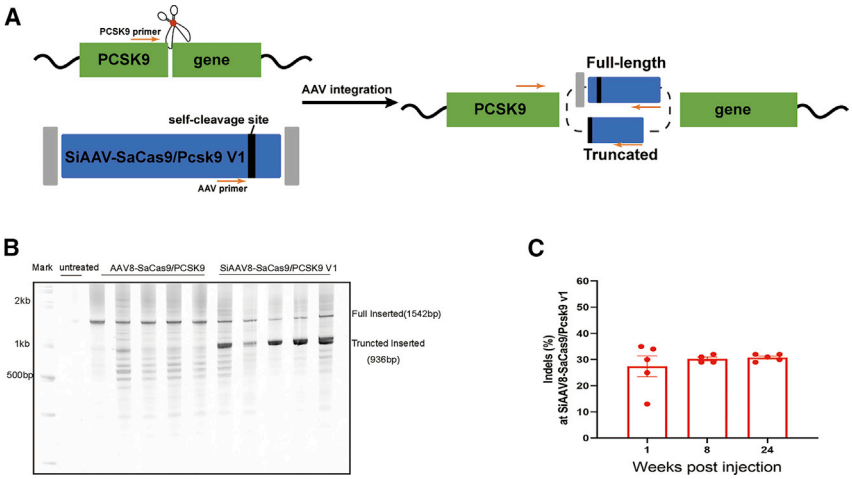

Figure 5. Characterization of AAV integration in the genomic loci and the indels at the AAV genome

(A) Schematic of detecting the AAV vector integration into genomic loci (*PCSK9*) using PCR. (B) All injected AAV samples have full-length insertion at the *PCSK9* locus at 24 weeks. SiAAV8-SaCas9/Pcsk9 V1 samples had full-length AAV amplification bands and truncated AAV fragments. (C) Indels of SiAAV8-SaCas9/Pcsk9 V1 vector was detected at weeks 1, 8, and 24 via NGS. Mean ± SEM are shown.

In summary, we have developed an all-in-one self-cleavage AAV-CRISPR-Cas9 system to limit the duration of Cas9 expression. This system can efficiently edit genomic loci while achieving self-targeted cleavage of the AAV vector and significantly reduce the off-target effect and immune effect of CRISPR-Cas9. Including the self-cleavage strategy in gene-editing approaches has the potential to increase the safety profile of AAV-delivered genome-editing nucleases and thereby promote the clinical transformation of AAV-CRISPR-Cas9 technology.

MATERIALS AND METHODS

Plasmid construction

Three sgRNA sequences located in the murine *PCSK9* exons 3 were selected. These target sequences were cloned into pX602 plasmid (Addgene plasmid #61593). The pAAV-SaCas9/Pcks9 gene-targeting vector was constructed by infusion cloning, which consists of a liver-specific hAAT promoter, SaCas9, and a U6-*PCSK9* sgRNA2 that specifically targets a region in the exons 3 of murine *PCSK9*. The two self-cleavage candidate plasmids were constructed as follows. Briefly, the self-cleavage sequences were included in the primers. The primer pairs flanked the insertion site of the pAAV-SaCas9/Pcsk9. The insertion site was amplificated by PCR. Then, the pAAV-SaCas9/Pcsk9 was double-digested by a restriction enzyme at the insertion site, followed by T4 ligase treatment with PCR amplicon. The sgRNAs and primers sequences of vector construction are shown in Table S1. All plasmid constructions were verified by sequencing.

AAV vector production

All AAV8 vectors were produced by triple plasmid transfection of human embryonic kidney 293 cells (ATCC). The genome titer (genome copies mL^{-1}) of AAV8 vectors was carried out by qPCR (Roche, Cat# 06402682001). The presence of endotoxins in AAV8 vector production was detected with LAL Chromogenic Endotoxin Quantitation Kit (Xiamen Bioendo Technology, China, Cat# EC32545S) according to the manufacturer's manual. All recombinant AAV production plasmids were generated by using an EndoFree Plasmid Megaprep Kit (QIAGEN, Hilden, Germany). The sequences of primers were listed in Table S1.

Cell culture and transfection

H2.35 cells (ATCC), Huh7 cells (ATCC), HCCLM3 cells (ATCC), and SMCC-7721 cells (ATCC) were maintained in DMEM medium supplemented with 10% fetal bovine serum (FBS) and cultured at 37°C with 5% CO_2. For *in vitro* target verification, the TransIT-X2 system (Mirus) transfection reagent was used to co-transfect a plasmid containing SaCas9 and sgRNA and a plasmid expressing GFP and puromycin resistance into H2.35 cells, according to the manufacturer's recommendations. Transfected cells were selected by puromycin (1 μg/mL) for 3 days to enrich transfected cells.

Genomic DNA extraction and SURVEYOR assay

Genomic DNA was extracted from transient transfected H2.35 cells by using the QuickExtract DNA Extraction Solution (Epicenter Biotechnologies). SURVEYOR nuclease assay (Transgenomics) was performed as described previously[38] to determine the genome efficiency of individual sgRNA using the PCR primers listed in Table S1.

Viral genome copy number analysis

Genomic DNA from Huh7 cell, HCCLM3 cell, and SMCC-7721 cell infected by AAV8 virus were extracted as described above. The viral genome copy number was calculated by qPCR (Roche, Cat# 06402682001). The primer sequences for qPCR were described in Table S1.

Western blot analysis

The cells and liver tissues were lysed in radioimmunoprecipitation assay (RIPA) lysis buffer and analyzed by western blot. SaCas9 protein was detected by rabbit hemagglutinin (HA)-tag antibody (Cat# 51064-2-AP, Proteintech, 1:1,000). Rabbit anti-β-actin antibody (Cat# AC026, ABclonal, 1:100,000) was used to detect β-actin. Goat anti-rabbit immunoglobulin G (IgG) and horseradish peroxidase (HRP)-linked antibody were used (Cat#7074, Cell Signaling Technology, 1:100,000). Image analysis of blots was performed with iBright CL1000 imaging systems (Invitrogen, Thermo Fisher Scientific).

Animal studies

All mice were acquired from the Beijing Huafukang Biotechnology (China). AAV vectors were delivered to 4- to 6-week-old male C57/BL6 mice (n = 36) intravenously via tail vein injection. The dosage of AAV was adjusted to 2×10^{11} genome copies per mouse with

sterile phosphate-buffered saline (PBS) before the injection. Untreated mice (n = 5) with PBS served as controls. For testing the serum levels of PCSK9 and total cholesterol, the animals were fasted overnight before blood collection by retro-orbital bleeding. Blood was collected at various time points before and after tail vein delivery of AAV vector. Then it was centrifuged to separate the serum and stored at −80°C for subsequent analysis. At 1, 8, or 24 weeks post treatment, a fraction of mice were euthanized and liver samples were harvested for subsequent analysis. A portion of the liver tissue was removed and fixed in a 4% paraformaldehyde solution for histological analysis, while the remaining tissue was cut into small pieces and frozen for subsequent experiments. All animal procedures were approved by the Institutional Animal Care and Concern Committee at Sichuan University, and animal care was in accordance with the committee's guidelines.

On-target and off-target mutagenesis analyses

The genomic DNA were extracted from mouse liver tissues 1, 8, and 24 weeks following vector administration to measure genome-editing efficiency *in vivo*. After nest PCR amplification with primers flanking the on- and off-target loci, PCR products were used for an NGS assay. On-target and off-target mutagenesis analyses were performed as previously described.[39] The oligonucleotide primer sequences used to amplify relevant sequences by nested PCR are described in Tables S2 and S3.

ELISA

Levels of PCSK9 in serum are detected by the mouse proprotein convertase 9/PCSK9 Quantikine ELISA kit (MPC-900, R&D Systems) according to the manufacturer's instructions. The serum samples were diluted with the Calibrator diluent at a ratio of 1:200 and then added to the microplate wells coated with capture antibody in advance and bound for 2 h onto microplate wells. The wells were washed 3 times with the washing buffer for 5 min each. The samples were then sequentially incubated with the PCSK9 conjugate followed by the PCSK9 substrate solution, with the washing process repeated 3 times between each step. Finally, the content of Pcsk9 in serum was evaluated using a microplate reader.

AAV8 and SaCas9 ELISAs were performed as follows.[37] AAV8 virus and SaCas9 protein were diluted with coating buffer, respectively. Microwell plates then were coated with 1×10^9 GC/100 μL AAV8 virus and 0.5 μg/100 μL SaCas9 protein per well and incubated at 4°C overnight. The plates were washed 3 times for 5 min with 300 μL of washing buffer and subsequently blocked with 300 μL of BSA blocking solution (Bethyl) at room temperature for 2 h. The washing was repeated again. Serum samples were added at 1:40 dilution and the plates were incubated at 37°C for 4 h. The wells were washed 3 times for 5 min each and 100 μL of HRP-labeled goat anti-mouse IgG1, which was diluted with BSA blocking solution at a ratio of 1:100,000, was added to each well. After 1 h incubation at room temperature, the wells were washed 4 times for 5 min each and then 100 μL of 3,3′,5,5′-tetramethylbenzidine (TMB) substrate was added to each well and incubated for 15 min at room temperature in the dark. The optical density (OD450) at 450 nm was measured using a microplate reader after adding 100 μL of stop solution to each well.

Histopathology

The paraffin-embedded liver samples were cut into 6 μm sections and then tissue sections were processed and H&E stained according to standard procedures. The sections were analyzed for any abnormalities compared to the livers of untreated animals.

AAV vector integration and indels analysis

In vivo possible vector integration with the self-inactivating system was measured using genomic DNA extracted from mouse liver tissues at 24 weeks following vector administration. After PCR amplification with primers flanking the genomic loci (*PCSK9*) and AAV vector, PCR products were separated with electrophoresis on Tris-borate-EDTA (TBE) gels (Invitrogen, Cat#19050647). To detect the indels of self-inactivating AAV vectors, we designed primers on both sides of the self-cleavage site of AAV vector to amplify the target region for nest PCR. Purified PCR fragments were subjected to NGS. The sequences of primers were listed in Table S4.

Statistics

The values represent the mean ± SEM. Dunnett's test was used for statistical analysis, as shown in the figure legends. In all tests, $p < 0.05$ was considered significant. All statistical tests were performed using GraphPad Prism8.

SUPPLEMENTAL INFORMATION

Supplemental Information can be found online at https://doi.org/10.1016/j.omtm.2021.02.005.

ACKNOWLEDGMENTS

This work was supported by the Joint Funds of the National Natural Science Foundation of China (grant no. U19A2002), National Major Scientific and Technological Special Project for "Significant New Drugs Development" (no. 2018ZX09733001-005-002), and the Science and Technology Major Project of Sichuan province (no. 2017SZDZX0011).

AUTHOR CONTRIBUTIONS

Y.Y. conceived this study and designed the experiments. L.M. constructed the vectors. Q.L. and J.S. performed mouse studies. Q.L. performed indel and targeting efficiency analyses. Y.L. performed the ELISA assay. X.J. and Q.W. performed qPCR analysis. X.Z. performed histopathology assays. Q.L. wrote the manuscript. Y.Y. and H.D. edited the manuscript. All authors read and approved the final manuscript.

DECLARATION OF INTERESTS

The authors declare no competing interests.

REFERENCES

1. Mali, P., Esvelt, K.M., and Church, G.M. (2013). Cas9 as a versatile tool for engineering biology. Nat. Methods *10*, 957–963.

2. Jinek, M., Chylinski, K., Fonfara, I., Hauer, M., Doudna, J.A., and Charpentier, E. (2012). A programmable dual-RNA-guided DNA endonuclease in adaptive bacterial immunity. Science *337*, 816–821.

3. Gasiunas, G., Barrangou, R., Horvath, P., and Siksnys, V. (2012). Cas9-crRNA ribonucleoprotein complex mediates specific DNA cleavage for adaptive immunity in bacteria. Proc. Natl. Acad. Sci. USA *109*, E2579–E2586.

4. Doudna, J.A., and Charpentier, E. (2014). Genome editing. The new frontier of genome engineering with CRISPR-Cas9. Science *346*, 1258096.

5. Anders, C., Niewoehner, O., Duerst, A., and Jinek, M. (2014). Structural basis of PAM-dependent target DNA recognition by the Cas9 endonuclease. Nature *513*, 569–573.

6. Cong, L., Ran, F.A., Cox, D., Lin, S., Barretto, R., Habib, N., Hsu, P.D., Wu, X., Jiang, W., Marraffini, L.A., and Zhang, F. (2013). Multiplex genome engineering using CRISPR/Cas systems. Science *339*, 819–823.

7. Mali, P., Yang, L., Esvelt, K.M., Aach, J., Guell, M., DiCarlo, J.E., Norville, J.E., and Church, G.M. (2013). RNA-guided human genome engineering via Cas9. Science *339*, 823–826.

8. Kotterman, M.A., Chalberg, T.W., and Schaffer, D.V. (2015). Viral Vectors for Gene Therapy: Translational and Clinical Outlook. Annu. Rev. Biomed. Eng. *17*, 63–89.

9. Mingozzi, F., and High, K.A. (2011). Therapeutic in vivo gene transfer for genetic disease using AAV: progress and challenges. Nat. Rev. Genet. *12*, 341–355.

10. Zincarelli, C., Soltys, S., Rengo, G., and Rabinowitz, J.E. (2008). Analysis of AAV serotypes 1-9 mediated gene expression and tropism in mice after systemic injection. Mol. Ther. *16*, 1073–1080.

11. Lau, C.H., and Suh, Y. (2017). *In vivo* genome editing in animals using AAV-CRISPR system: applications to translational research of human disease. F1000Res. *6*, 2153.

12. Li, C., Psatha, N., Gil, S., Wang, H., Papayannopoulou, T., and Lieber, A. (2018). HDAd5/35^{++} Adenovirus Vector Expressing Anti-CRISPR Peptides Decreases CRISPR-Cas9 Toxicity in Human Hematopoietic Stem Cells. Mol. Ther. Methods Clin. Dev. *9*, 390–401.

13. Ihry, R.J., Worringer, K.A., Salick, M.R., Frias, E., Ho, D., Theriault, K., Kommineni, S., Chen, J., Sondey, M., Ye, C., et al. (2018). p53 inhibits CRISPR-Cas9 engineering in human pluripotent stem cells. Nat. Med. *24*, 939–946.

14. Kosicki, M., Tomberg, K., and Bradley, A. (2018). Repair of double-strand breaks induced by CRISPR-Cas9 leads to large deletions and complex rearrangements. Nat. Biotechnol. *36*, 765–771.

15. Cohen, J., Pertsemlidis, A., Kotowski, I.K., Graham, R., Garcia, C.K., and Hobbs, H.H. (2005). Low LDL cholesterol in individuals of African descent resulting from frequent nonsense mutations in PCSK9. Nat. Genet. *37*, 161–165.

16. Cohen, J.C., Boerwinkle, E., Mosley, T.H., Jr., and Hobbs, H.H. (2006). Sequence variations in PCSK9, low LDL, and protection against coronary heart disease. N. Engl. J. Med. *354*, 1264–1272.

17. Ding, Q., Strong, A., Patel, K.M., Ng, S.L., Gosis, B.S., Regan, S.N., Cowan, C.A., Rader, D.J., and Musunuru, K. (2014). Permanent alteration of PCSK9 with in vivo CRISPR-Cas9 genome editing. Circ. Res. *115*, 488–492.

18. Ran, F.A., Cong, L., Yan, W.X., Scott, D.A., Gootenberg, J.S., Kriz, A.J., Zetsche, B., Shalem, O., Wu, X., Makarova, K.S., et al. (2015). In vivo genome editing using Staphylococcus aureus Cas9. Nature *520*, 186–191.

19. Chadwick, A.C., Wang, X., and Musunuru, K. (2017). In Vivo Base Editing of PCSK9 (Proprotein Convertase Subtilisin/Kexin Type 9) as a Therapeutic Alternative to Genome Editing. Arterioscler. Thromb. Vasc. Biol. *37*, 1741–1747.

20. Yin, H., Song, C.Q., Suresh, S., Wu, Q., Walsh, S., Rhym, L.H., Mintzer, E., Bolukbasi, M.F., Zhu, L.J., Kauffman, K., et al. (2017). Structure-guided chemical modification of guide RNA enables potent non-viral in vivo genome editing. Nat. Biotechnol. *35*, 1179–1187.

21. Miller, D.G., Petek, L.M., and Russell, D.W. (2003). Human gene targeting by adeno-associated virus vectors is enhanced by DNA double-strand breaks. Mol. Cell. Biol. *23*, 3550–3557.

22. Hanlon, K.S., Kleinstiver, B.P., Garcia, S.P., Zaborowski, M.P., Volak, A., Spirig, S.E., Muller, A., Sousa, A.A., Tsai, S.Q., Bengtsson, N.E., et al. (2019). High levels of AAV vector integration into CRISPR-induced DNA breaks. Nat. Commun. *10*, 4439.

23. Zetsche, B., Volz, S.E., and Zhang, F. (2015). A split-Cas9 architecture for inducible genome editing and transcription modulation. Nat. Biotechnol. *33*, 139–142.

24. Kleinjan, D.A., Wardrope, C., Nga Sou, S., and Rosser, S.J. (2017). Drug-tunable multidimensional synthetic gene control using inducible degron-tagged dCas9 effectors. Nat. Commun. *8*, 1191.

25. Senturk, S., Shirole, N.H., Nowak, D.G., Corbo, V., Pal, D., Vaughan, A., Tuveson, D.A., Trotman, L.C., Kinney, J.B., and Sordella, R. (2017). Rapid and tunable method to temporally control gene editing based on conditional Cas9 stabilization. Nat. Commun. *8*, 14370.

26. Maji, B., Moore, C.L., Zetsche, B., Volz, S.E., Zhang, F., Shoulders, M.D., and Choudhary, A. (2017). Multidimensional chemical control of CRISPR-Cas9. Nat. Chem. Biol. *13*, 9–11.

27. Dow, L.E., Fisher, J., O'Rourke, K.P., Muley, A., Kastenhuber, E.R., Livshits, G., Tschaharganeh, D.F., Socci, N.D., and Lowe, S.W. (2015). Inducible in vivo genome editing with CRISPR-Cas9. Nat. Biotechnol. *33*, 390–394.

28. Harrington, L.B., Doxzen, K.W., Ma, E., Liu, J.J., Knott, G.J., Edraki, A., Garcia, B., Amrani, N., Chen, J.S., Cofsky, J.C., et al. (2017). A Broad-Spectrum Inhibitor of CRISPR-Cas9. Cell *170*, 1224–1233.e15.

29. Huang, X., Chen, Z., and Liu, Y. (2020). RNAi-mediated control of CRISPR functions. Theranostics *10*, 6661–6673.

30. Merienne, N., Vachey, G., de Longprez, L., Meunier, C., Zimmer, V., Perriard, G., Canales, M., Mathias, A., Herrgott, L., Beltraminelli, T., et al. (2017). The Self-Inactivating KamiCas9 System for the Editing of CNS Disease Genes. Cell Rep. *20*, 2980–2991.

31. Petris, G., Casini, A., Montagna, C., Lorenzin, F., Prandi, D., Romanel, A., Zasso, J., Conti, L., Demichelis, F., and Cereseto, A. (2017). Hit and go CAS9 delivered through a lentiviral based self-limiting circuit. Nat. Commun. *8*, 15334.

32. Baum, C., Kustikova, O., Modlich, U., Li, Z., and Fehse, B. (2006). Mutagenesis and oncogenesis by chromosomal insertion of gene transfer vectors. Hum. Gene Ther. *17*, 253–263.

33. Li, A., Lee, C.M., Hurley, A.E., Jarrett, K.E., De Giorgi, M., Lu, W., Balderrama, K.S., Doerfler, A.M., Deshmukh, H., Ray, A., et al. (2018). A Self-Deleting AAV-CRISPR System for *In Vivo* Genome Editing. Mol. Ther. Methods Clin. Dev. *12*, 111–122.

34. Ibraheim, R., Tai, P.W.L., Mir, A., Javeed, N., Wang, J., Rodríguez, T., Nelson, S., Khokhar, E., Mintzer, E., Maitland, S., et al. (2020). Precision Cas9 Genome Editing in vivo with All-in-one, Self-targeting AAV Vectors. bioRxiv *2020*, 333997.

35. Wang, D., Zhang, F., and Gao, G. (2020). CRISPR-Based Therapeutic Genome Editing: Strategies and In Vivo Delivery by AAV Vectors. Cell *181*, 136–150.

36. Chew, W.L., Tabebordbar, M., Cheng, J.K., Mali, P., Wu, E.Y., Ng, A.H., Zhu, K., Wagers, A.J., and Church, G.M. (2016). A multifunctional AAV-CRISPR-Cas9 and its host response. Nat. Methods *13*, 868–874.

37. Moreno, A.M., Palmer, N., Alemán, F., Chen, G., Pla, A., Jiang, N., Leong Chew, W., Law, M., and Mali, P. (2019). Immune-orthogonal orthologues of AAV capsids and of Cas9 circumvent the immune response to the administration of gene therapy. Nat. Biomed. Eng. *3*, 806–816.

38. Ran, F.A., Hsu, P.D., Wright, J., Agarwala, V., Scott, D.A., and Zhang, F. (2013). Genome engineering using the CRISPR-Cas9 system. Nat. Protoc. *8*, 2281–2308.

39. Wang, Q., Zhong, X., Li, Q., Su, J., Liu, Y., Mo, L., Deng, H., and Yang, Y. (2020). CRISPR-Cas9-Mediated *In Vivo* Gene Integration at the Albumin Locus Recovers Hemostasis in Neonatal and Adult Hemophilia B Mice. Mol. Ther. Methods Clin. Dev. *18*, 520–531.

OMTM, Volume *20*

Supplemental information

In vivo PCSK9 gene editing using an all-in-one self-cleavage AAV-CRISPR system

Qian Li, Jing Su, Yi Liu, Xiu Jin, Xiaomei Zhong, Li Mo, Qingnan Wang, Hongxin Deng, and Yang Yang

Supplemental Table 1. Primers and sequences for construction of plasmids and analysis of gene target and expression.

Name	Sequence	Note
Pcsk9 sgRNA1_Fwd	CACCGATGCTCTGGGCGAAGACAA	Pcsk9 target sequence 1
Pcsk9 sgRNA1_Rev	AAACTTGTCTTCGCCCAGAGCATC	
Pcsk9 sgRNA2_Fwd	CACCGAGCATCCCATGGAACCTGGA	Pcsk9 target sequence 2
Pcsk9 sgRNA2_Rev	AAACTCCAGGTTCCATGGGATGCTC	
Pcsk9 sgRNA3_Fwd	CACCGATAATTCGCTCCAGGTTCCA	Pcsk9 target sequence 3
Pcsk9 sgRNA3_Rev	AAACTGGAACCTGGAGCGAATTATC	
Pcsk9_ P1Fwd	GATGCCTCCTATTAGCCAAA	Pcsk9 PCR for Surveyor and NGS
Pcsk9_ P1Rev	TGGTCATGGAGTCTCTTCAC	
Pcsk9_ P2Fwd	AATCCAGAGAGTGGAATAGAGAACC	
Pcsk9_ P2Rev	AGCAATGCAGAGAGCACAGA	
BGH_PA_qPCR_Fwd	GCCAGCCATCTGTTGT	Primers and probe for AAV titer and genome copies number assay
BGH_PA_qPCR_Rev	GGAGTGGCACCTTCCA	
BGH_PA_qPCR_Probe	TCCCCCGTGCCTTCCTTGACC	

Supplemental Table 2. Off-target analysis. Potential off-target sequences for Pcsk9 sgRNA2 identified and scored by Benchling's off-target analysis.

ID	Sequence	PAM	Score	Chromosome	Strand	Position	Mismatches	On-target
sgRNA2	AGCATCCCATGGAACCTGGA	GCGAA	100.000	chr4	-1	106456915	0	
OT1	AGCATCCCATAGAACCTGTA	TAGAA	1.885	chr9	1	112468999	2	FALSE
OT2	AGCAGCCCATGAAACCTGGT	GTGAA	0.480	chr9	1	89762172	3	FALSE
OT3	AGCAACCCAAGGAACCTGGG	GTGGG	0.480	chr2	1	174575620	3	FALSE
OT4	AGGATCCCTTGGAACTTGGA	GAGGA	0.437	chr1	-1	177702483	3	FALSE
OT5	AGCATCTCATTGAACCTGGG	ATGGG	0.437	chr1	-1	175960029	3	FALSE
OT6	AGCCTCCCATGGAAGGTGGA	GTGAG	0.419	chr5	1	110977460	3	FALSE
OT7	AGCATTCCATGGAATCTAGA	CTGGA	0.419	chr5	-1	34608483	3	FALSE
OT8	AGGGTCCCATGGAAACTGGA	TGGAA	0.419	chr17	-1	49827739	3	FALSE
OT9	AGCATCCCAAGGGACCTGGC	TGGGG	0.386	chr19	1	29045533	3	FALSE
OT10	AGCATCCCAGGAAACCTGAA	ATGAA	0.372	chr2	1	160149048	3	FALSE

Supplemental Table 3. PCR primer sequences for detecting potential off-target effects by NGS assay.

Primer Name	Sequence	Note
OT1_P1Fwd	CTTGCACACTATAGTTATGTCT	Primers for OT1
OT1_P1Rev	GACCTTCACACATAAATAGATG	
OT1_P2Fwd	AAATTGCTCTCTATTCACTTGG	
OT1_P2Rev	AAGAGCAGGAAAGATAACTG	
OT2_P1Fwd	GTAAAGGAGCATATGTGTACA	Primers for OT2
OT2_P1Rev	ATTCACGATTCAAACTCCAG	
OT2_P2Fwd	TTCTCTGAATTCTTGAAGCT	
OT2_P2Rev	ATTTGACAATGAATTGCTGG	
OT3_P1Fwd	GTTTGTCTAACAGGCTGTGA	Primers for OT3
OT3_P1Rev	CACACAAGGAAGATTCAGAA	
OT3_P2Fwd	GATGTGAGTCCTTTCATCTA	
OT3_P2Rev	CTAAAGTCACATGACAAGGA	
OT4_P1Fwd	CTGCAAGCAACAACATAGAC	Primers for OT4
OT4_P1Rev	TATAAAACCACAGAGGGAAG	
OT4_P2Fwd	ATCTTAGCCTACACATTGAG	
OT4_P2Rev	ATTGCAGTTCTTAGATGGCT	
OT5_P1Fwd	TGTTTGCATTACAGGAGCTG	Primers for OT5
OT5_P1Rev	GATGTCTTTGAGTCTCGCAG	
OT5_P2Fwd	ATAGAATTTGGAGAGAGAAACC	
OT5_P2Rev	TTCTTAGTCGGATTGGTTGG	
OT6_P1Fwd	GTGTCGATGATGTGTGTGGA	Primers for OT6
OT6_P1Rev	ACACACCTGTTGACTGCCAT	
OT6_P2Fwd	CTCCAGATACTAAACACAATG	
OT6_P2Rev	GCATTCAACATTCTTCATCA	
OT7_P1Fwd	CATCTATATTAGATACCATCACACC	Primers for OT7
OT7_P1Rev	GCAAAAGGTATTACACACAG	
OT7_P2Fwd	CTCAGGGATTTTATAGTGCT	
OT7_P2Rev	CTGTAATGAGGTTGGACAGC	
OT8_P1Fwd	CAGCACTACTATTGGTCTTC	Primers for OT8
OT8_P1Rev	TTCTTATACACTGGTCCCCT	
OT8_P2Fwd	CACTTTGGTCAATTTTGCAG	
OT8_P2Rev	AACTGGAGCTACAGAGGGTT	
OT9_P1Fwd	ACATCTCATTTGCTTGATTC	Primers for OT9
OT9_P1Rev	GAGCTGAACACACAAAGTTG	
OT9_P2Fwd	AACATCTGTGGGAACAATCT	
OT9_P2Rev	TTTAACAGGGTCTCAGACAG	
OT10_P1Fwd	TCCACACGGGTAAGGAGGAA	Primers for OT10
OT10_P1Rev	GCACATTCCAATGAGCCTGT	
OT10_P2Fwd	CCGATGACAATCAAAGCCAG	
OT10_P2Rev	TTGCTGAGTCATCACTTGGA	

Supplemental Table4. PCR primer sequences for detecting AAV integration and indels in AAV genome.

Name	Sequence	Note
Pcsk9-5'_Fwd	GATGCCTCCTATTAGCCAAA	AAV integration sequence
AAV-3'_Rev	GTACAGCACAGACATTCTGG	
AAV-indel_ P1Fwd	ATACGTCGGAACTGCTCTGCA	PCR for indels in AAV genome and NGS
AAV-indel_ P1Rev	AGGGCCTATTTCCCATGA	
AAV-indel_ P2Fwd	TCGACTGTGCCTTCTAGTTG	
AAV-indel_ P2Rev	GGCTGTTAGAGAGATAATTGG	

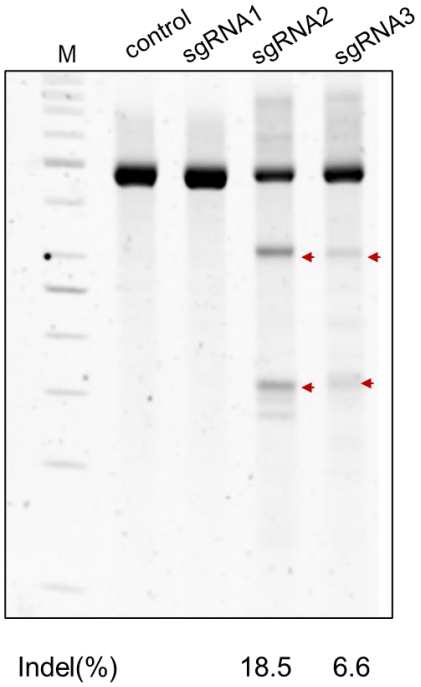

Supplemental Figure 1 Selection of optimal self-cleavage gRNA *in vitro*. Validation of three candidate gRNA plasmids in the H2.35 mouse cell line by transient transfection and SURVEYOR nuclease assays. Arrows denote SURVEYOR nuclease cleaved fragments of the PCSK9 PCR products.

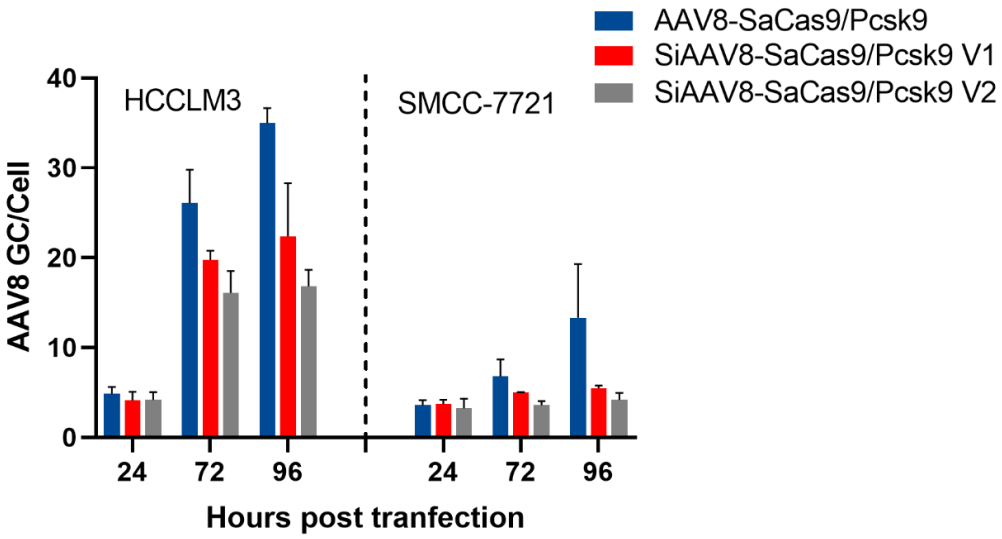

Supplemental Figure 2 The genome copy number of virus in both self-cleavage vector groups increased slowly with time. Quantitative analysis of virus genome copy number at different time points after infection with HCCLM3 cell line and SMCC-7721 cell line by qPCR.